KOMPUTASI: JURNAL ILMIAH ILMU KOMPUTER DAN MATEMATIKA
VOL. 22 (2) (2025), 10-19, p-ISSN: 693-7554, e-ISSN:2654-3990

Numerical Verification of the Order of Accuracy of a Runge-Kutta-Fehlberg Method in Solving an SEIR Model

Lintang Kinanthi Widi[1*], Sudi Mungkasi[2]

[1,2] Department of Mathematics, Faculty of Science and Technology, Sanata Dharma University, Yogyakarta, 55281, Indonesia
[*]Corresponding author. E-mail address: lintangkinanthiw@gmail.com

Abstract

A Runge-Kutta-Fehlberg method (RKF45) is considered to solve an SEIR (Susceptible-Exposed-Infected-Recovered) mathematical model for infectious disease transmission. This numerical method is of the Runge-Kutta class, and has theoretical order of accuracy four and five depending on the involved formulations. We limit our problem to the RKF45 formula having theoretical order five. It is important to understand the behavior of RKF45 in solving an initial value problem, especially when implemented for real problems. In this paper, we take an SEIR mathematical model in our case, because this model is applicable in the prediction of infectious disease transmission in real life. Our research method is quantitative. We record the errors of numerical simulations. From the error values, we determine the numerical order of accuracy. Our research results show that RKF45 produces numerical order of accuracy five for the time step is sufficiently small. Therefore, the numerical order of accuracy matches with the theoretical one.

Keywords: *Numerical method; order of accuracy; Runge-Kutta-Fehlberg method; SEIR model; verification*

1. Introduction

Numerical methods have been important tools for solving various mathematical problems [1]. A mathematical problem itself is usually occurred from a real-world problem. This means that numerical methods are useful for solving real-world problems [2].

In this paper we consider a Runge-Kutta-Fehlberg method (RKF45) [3], which is applicable for solving an initial value problem of ordinary differential equations, such as an SEIR (Susceptible-Exposed-Infected-Recovered) mathematical model [4]. RKF45 method and SEIR model are of our interest, because RKF45 is simple to program (as it is a one-step method) and it has the order of accuracy four or five, and SEIR model is useful in modelling the real-world infectious disease transmission. In this paper, we limit our RKF45 method to be the one having the fifth order of accuracy.

The theoretical order of accuracy of a numerical method needs to be verified numerically. This is important, because modelers must know the behavior of the numerical method when implemented. Understanding the numerical behavior of the method is useful, so that the analysis of numerical results will be more accurate [5]-[7]. This will aid in understanding the solutions of the real-world problem through mathematical modeling and its solutions [8]-[13]. Based on these grounds, this paper aims to verify numerically the fifth order RKF45 method in solving a SEIR model.

The rest of this paper consists of Section 2 recalling the mathematical model, Section 3 writing the numerical method, Section 4 containing results and discussion, and Section 5 remarking some conclusions.

2. Mathematical Model

The SEIR model for infectious disease transmission consists of four compartments of the population, namely, S (Susceptible) subpopulation, E (Exposed) subpopulation, I (Infected) subpopulation, and R (Recovered) subpopulation. In this paper we consider the improved SEIR model proposed by Jiao et al. [4]. The schematic diagram of the model is illustrated in Figure 1.

[*]**Corresponding author**. *E-mail address: lintangkinanthiw@gmail.com*
Received: 26 March 2025, Accepted: 31 July 2025 and available online 31 July 2025
DOI: https://doi.org/10.33751/komputasi.v19i2.5260

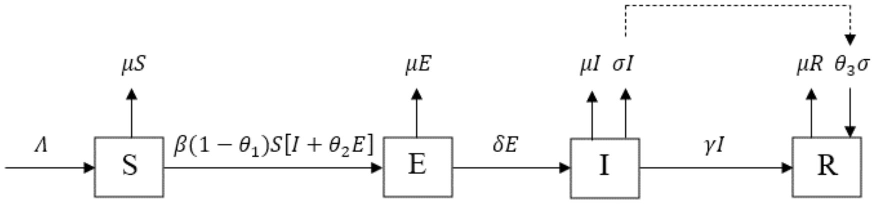

Figure 1. Schematic diagram for the SEIR model.

The SEIR model is expressed as a system of ordinary differential equation as follows [4]:

$$\begin{cases} \dfrac{dS}{dt} = \Lambda - \beta(1-\theta_1)S(t)[I(t)+\theta_2 E(t)] - \mu S(t), \\ \dfrac{dE}{dt} = \beta(1-\theta_1)S(t)[I(t)+\theta_2 E(t)] - (\delta+\mu)E(t), \\ \dfrac{dI}{dt} = \delta E(t) - (\gamma+\sigma+\mu)I(t), \\ \dfrac{dR}{dt} = (\gamma+\theta_3\sigma)I - \mu R(t). \end{cases} \tag{1}$$

In this model, t is the time variable and $\Lambda, \beta, \theta_1, \theta_2, \theta_3, \mu, \delta, \gamma, \sigma$ are parameters. In addition, S, E, I, R are dependent on t. More explanation and properties of this model are available in the work of Jiao et al. [4].

3. Methods

The numerical method for solving the problem is the fifth-order RKF45. Suppose we are given the initial value problem:

$$\frac{dy}{dt} = f(t,y)$$
$$y(t_0) = y_0$$

then the fifth-order RKF45 method takes the following scheme [3]:

$$y_{i+1} = y_i + \frac{16}{135}k_1 + \frac{6656}{12825}k_3 + \frac{28561}{56430}k_4 - \frac{9}{50}k_5 + \frac{2}{55}k_6 \tag{2}$$

where:

$$\begin{aligned} k_1 &= h\,f(t_i,\, y_i), \\ k_2 &= h\,f\left(t_i + \frac{1}{4}h,\, y_i + \frac{1}{4}k_1\right), \\ k_3 &= h\,f\left(t_i + \frac{3}{8}h,\, y_i + \frac{3}{32}k_1 + \frac{9}{32}k_2\right), \\ k_4 &= h\,f\left(t_i + \frac{12}{13}h,\, y_i + \frac{1932}{2197}k_1 - \frac{7200}{2197}k_2 + \frac{7296}{2197}k_3\right), \\ k_5 &= h\,f\left(t_i + h,\, y_i + \frac{439}{216}k_1 - 8k_2 + \frac{3680}{513}k_3 - \frac{845}{4104}k_4\right), \\ k_6 &= h\,f\left(t_i + \frac{1}{2}h,\, y_i - \frac{8}{27}k_1 + 2k_2 - \frac{3544}{2565}k_3 + \frac{1859}{4104}k_4 - \frac{11}{40}k_5\right). \end{aligned} \tag{3}$$

Therefore, the RKF45 scheme for solving the model is:

$$\begin{aligned} S_{i+1} &= S_i + \left(\frac{16}{135}k_{1,S} + \frac{6656}{12825}k_{3,S} + \frac{28561}{56430}k_{4,S} - \frac{9}{50}k_{5,S} + \frac{2}{55}k_{6,S}\right) \\ E_{i+1} &= E_i + \left(\frac{16}{135}k_{1,E} + \frac{6656}{12825}k_{3,E} + \frac{28561}{56430}k_{4,E} - \frac{9}{50}k_{5,E} + \frac{2}{55}k_{6,E}\right) \\ I_{i+1} &= I_i + \left(\frac{16}{135}k_{1,I} + \frac{6656}{12825}k_{3,I} + \frac{28561}{56430}k_{4,I} - \frac{9}{50}k_{5,I} + \frac{2}{55}k_{6,I}\right) \\ R_{i+1} &= R_i + \left(\frac{16}{135}k_{1,R} + \frac{6656}{12825}k_{3,R} + \frac{28561}{56430}k_{4,R} - \frac{9}{50}k_{5,R} + \frac{2}{55}k_{6,R}\right) \end{aligned} \tag{4}$$

with the $k_1, k_2, k_3, k_4, k_5, k_6$ values are as follows:

1. The k_1 values are given by:

$$
\begin{aligned}
k_{1,S} &= h * \{\Lambda - \beta(1-\theta_1)S_i[I_i + \theta_2 E_i] - \mu S_i\} \\
k_{1,E} &= h * \{\beta(1-\theta_1)S_i[I_i + \theta_2 E_i] - (\delta + \mu)E_i\} \\
k_{1,I} &= h * \{\delta E_i - (\gamma + \sigma + \mu)I_i\} \\
k_{1,R} &= h * \{(\gamma + \theta_3\sigma)I_i - \mu R_i\}
\end{aligned}
\tag{5}
$$

2. The k_2 values are given by:

$$
\begin{aligned}
k_{2,S} &= h * \Big\{\Lambda - \beta(1-\theta_1)\left(S_i + \frac{1}{4}k_{1,S}\right)\left[\left(I_i + \frac{1}{4}k_{1,I}\right) + \theta_2\left(E_i + \frac{1}{4}k_{1,E}\right)\right] \\
&\qquad - \mu\left(S_i + \frac{1}{4}k_{1,S}\right)\Big\} \\
k_{2,E} &= h * \Big\{\beta(1-\theta_1)\left(S_i + \frac{1}{4}k_{1,S}\right)\left[\left(I_i + \frac{1}{4}k_{1,I}\right) + \theta_2\left(E_i + \frac{1}{4}k_{1,E}\right)\right] \\
&\qquad - (\delta + \mu)\left(E_i + \frac{1}{4}k_{1,E}\right)\Big\} \\
k_{2,I} &= h * \left\{\delta\left(E_i + \frac{1}{4}k_{1,E}\right) - (\gamma + \sigma + \mu)\left(I_i + \frac{1}{4}k_{1,I}\right)\right\} \\
k_{2R} &= h * \left\{(\gamma + \theta_3\sigma)\left(I_i + \frac{1}{4}k_{1,I}\right) - \mu\left(R_i + \frac{1}{4}k_{1,R}\right)\right\}
\end{aligned}
\tag{6}
$$

3. The k_3 values are given by:

$$
\begin{aligned}
k_{3,S} &= h * \Big\{\Lambda - \beta(1-\theta_1)\left(S_i + \frac{3}{32}k_{1,S} + \frac{9}{32}k_{2,S}\right)\Big[\left(I_i + \frac{3}{32}k_{1,I} + \frac{9}{32}k_{2,I}\right) \\
&\qquad + \theta_2\left(E_i + \frac{3}{32}k_{1,E} + \frac{9}{32}k_{2,E}\right)\Big] - \mu\left(S_i + \frac{3}{32}k_{1,S} + \frac{9}{32}k_{2,S}\right)\Big\} \\
k_{3,E} &= h * \Big\{\beta(1-\theta_1)\left(S_i + \frac{3}{32}k_{1,S} + \frac{9}{32}k_{2,S}\right)\Big[\left(I_i + \frac{3}{32}k_{1,I} + \frac{9}{32}k_{2,I}\right) \\
&\qquad + \theta_2\left(E_i + \frac{3}{32}k_{1,E} + \frac{9}{32}k_{2,E}\right)\Big] - (\delta + \mu)\left(E_i + \frac{3}{32}k_{1,E} + \frac{9}{32}k_{2,E}\right)\Big\} \\
k_{3,I} &= h * \left\{\delta\left(E_i + \frac{3}{32}k_{1,E} + \frac{9}{32}k_{2,E}\right) - (\gamma + \sigma + \mu)\left(I_i + \frac{3}{32}k_{1,I} + \frac{9}{32}k_{2,I}\right)\right\} \\
k_{3R} &= h * \left\{(\gamma + \theta_3\sigma)\left(I_i + \frac{3}{32}k_{1,I} + \frac{9}{32}k_{2,I}\right) - \mu\left(R_i + \frac{3}{32}k_{1,R} + \frac{9}{32}k_{2,R}\right)\right\}
\end{aligned}
\tag{7}
$$

4. The k_4 values are given by:

$$
\begin{aligned}
k_{4,S} &= h * \Big\{\Lambda - \beta(1-\theta_1)\Big(S_i + \frac{1932}{2197}k_{1,S} - \frac{7200}{2197}k_{2,S} \\
&\qquad + \frac{7296}{2197}k_{3,S}\Big)\Big[\left(I_i + \frac{1932}{2197}k_{1,I} - \frac{7200}{2197}k_{2,I} + \frac{7296}{2197}k_{3,I}\right) \\
&\qquad + \theta_2\left(E_i + \frac{1932}{2197}k_{1,E} - \frac{7200}{2197}k_{2,E} + \frac{7296}{2197}k_{3,E}\right)\Big] \\
&\qquad - \mu\left(S_i + \frac{1932}{2197}k_{1,S} - \frac{7200}{2197}k_{2,S} + \frac{7296}{2197}k_{3,S}\right)\Big\} \\
k_{4,E} &= h * \Big\{\beta(1-\theta_1)\Big(S_i + \frac{1932}{2197}k_{1,S} - \frac{7200}{2197}k_{2,S} \\
&\qquad + \frac{7296}{2197}k_{3,S}\Big)\Big[\left(I_i + \frac{1932}{2197}k_{1,I} - \frac{7200}{2197}k_{2,I} + \frac{7296}{2197}k_{3,I}\right) \\
&\qquad + \theta_2\left(E_i + \frac{1932}{2197}k_{1,E} - \frac{7200}{2197}k_{2,E} + \frac{7296}{2197}k_{3,E}\right)\Big] \\
&\qquad - (\delta + \mu)\left(E_i + \frac{1932}{2197}k_{1,E} - \frac{7200}{2197}k_{2,E} + \frac{7296}{2197}k_{3,E}\right)\Big\} \\
k_{4,I} &= h * \Big\{\delta\left(E_i + \frac{1932}{2197}k_{1,E} - \frac{7200}{2197}k_{2,E} + \frac{7296}{2197}k_{3,E}\right) \\
&\qquad - (\gamma + \sigma + \mu)\left(I_i + \frac{1932}{2197}k_{1,I} - \frac{7200}{2197}k_{2,I} + \frac{7296}{2197}k_{3,I}\right)\Big\} \\
k_{4,R} &= h * \Big\{(\gamma + \theta_3\sigma)\left(I_i + \frac{1932}{2197}k_{1,I} - \frac{7200}{2197}k_{2,I} + \frac{7296}{2197}k_{3,I}\right) \\
&\qquad - \mu\left(R_i + \frac{1932}{2197}k_{1,R} - \frac{7200}{2197}k_{2,R} + \frac{7296}{2197}k_{3,R}\right)\Big\}
\end{aligned}
\tag{8}
$$

5. The k_5 values are given by:

$$\begin{aligned}
k_{5,S} = h * \Big\{ &\Lambda - \beta(1-\theta_1)\left(S_i + \frac{439}{216}k_{1,S} - 8k_{2,S} + \frac{3680}{513}k_{3,S} \right.\\
&\left. - \frac{845}{4104}k_{4,S}\right)\left[\left(I_i + \frac{439}{216}k_{1,I} - 8k_{2,I} + \frac{3680}{513}k_{3,I} - \frac{845}{4104}k_{4,I}\right)\right.\\
&\left. + \theta_2\left(E_i + \frac{439}{216}k_{1,E} - 8k_{2,E} + \frac{3680}{513}k_{3,E} - \frac{845}{4104}k_{4,E}\right)\right]\\
&- \mu\left(S_i + \frac{439}{216}k_{1,S} - 8k_{2,S} + \frac{3680}{513}k_{3,S} - \frac{845}{4104}k_{4,S}\right)\Big\}\\
k_{5,E} = h * \Big\{ &\beta(1-\theta_1)\left(S_i + \frac{439}{216}k_{1,S} - 8k_{2,S} + \frac{3680}{513}k_{3,S} \right.\\
&\left. - \frac{845}{4104}k_{4,S}\right)\left[\left(I_i + \frac{439}{216}k_{1,I} - 8k_{2,I} + \frac{3680}{513}k_{3,I} - \frac{845}{4104}k_{4,I}\right)\right.\\
&\left. + \theta_2\left(E_i + \frac{439}{216}k_{1,E} - 8k_{2,E} + \frac{3680}{513}k_{3,E} - \frac{845}{4104}k_{4,E}\right)\right]\\
&- (\delta+\mu)\left(E_i + \frac{439}{216}k_{1,E} - 8k_{2,E} + \frac{3680}{513}k_{3,E} - \frac{845}{4104}k_{4,E}\right)\Big\}\\
k_{5,I} = h * \Big\{ &\delta\left(E_i + \frac{439}{216}k_{1,E} - 8k_{2,E} + \frac{3680}{513}k_{3,E} - \frac{845}{4104}k_{4,E}\right)\\
&- (\gamma+\sigma+\mu)\left(I_i + \frac{439}{216}k_{1,I} - 8k_{2,I} + \frac{3680}{513}k_{3,I} - \frac{845}{4104}k_{4,I}\right)\Big\}\\
k_{5,R} = h * \Big\{ &(\gamma+\theta_3\sigma)\left(I_i + \frac{439}{216}k_{1,I} - 8k_{2,I} + \frac{3680}{513}k_{3,I} - \frac{845}{4104}k_{4,I}\right)\\
&- \mu\left(R_i + \frac{439}{216}k_{1,R} - 8k_{2,R} + \frac{3680}{513}k_{3,R} - \frac{845}{4104}k_{4,R}\right)\Big\}
\end{aligned} \tag{9}$$

6. The k_6 values are given by:

$$\begin{aligned}
k_{6,S} = h * \Big\{ &\Lambda - \beta(1-\theta_1)\left(S_i - \frac{8}{27}k_{1,S} + 2k_{2,S} - \frac{3544}{2565}k_{3,S} + \frac{1859}{4104}k_{4,S} \right.\\
&\left. - \frac{11}{40}k_{5,S}\right)\left[\left(I_i - \frac{8}{27}k_{1,I} + 2k_{2,I} - \frac{3544}{2565}k_{3,I} + \frac{1859}{4104}k_{4,I} - \frac{11}{40}k_{5,I}\right)\right.\\
&\left. + \theta_2\left(E_i - \frac{8}{27}k_{1,E} + 2k_{2,E} - \frac{3544}{2565}k_{3,E} + \frac{1859}{4104}k_{4,E} - \frac{11}{40}k_{5,E}\right)\right]\\
&- \mu\left(S_i - \frac{8}{27}k_{1,S} + 2k_{2,S} - \frac{3544}{2565}k_{3,S} + \frac{1859}{4104}k_{4,S} - \frac{11}{40}k_{5,S}\right)\Big\}\\
k_{6,E} = h * \Big\{ &\beta(1-\theta_1)\left(S_i - \frac{8}{27}k_{1,S} + 2k_{2,S} - \frac{3544}{2565}k_{3,S} + \frac{1859}{4104}k_{4,S} \right.\\
&\left. - \frac{11}{40}k_{5,S}\right)\left[\left(I_i - \frac{8}{27}k_{1,I} + 2k_{2,I} - \frac{3544}{2565}k_{3,I} + \frac{1859}{4104}k_{4,I} - \frac{11}{40}k_{5,I}\right)\right.\\
&\left. + \theta_2\left(E_i - \frac{8}{27}k_{1,E} + 2k_{2,E} - \frac{3544}{2565}k_{3,E} + \frac{1859}{4104}k_{4,E} - \frac{11}{40}k_{5,E}\right)\right]\\
&- (\delta+\mu)\left(E_i - \frac{8}{27}k_{1,E} + 2k_{2,E} - \frac{3544}{2565}k_{3,E} + \frac{1859}{4104}k_{4,E} - \frac{11}{40}k_{5,E}\right)\Big\}\\
k_{6,I} = h * \Big\{ &\delta\left(E_i - \frac{8}{27}k_{1,E} + 2k_{2,E} - \frac{3544}{2565}k_{3,E} + \frac{1859}{4104}k_{4,E} - \frac{11}{40}k_{5,E}\right)\\
&- (\gamma+\sigma+\mu)\left(I_i - \frac{8}{27}k_{1,I} + 2k_{2,I} - \frac{3544}{2565}k_{3,I} + \frac{1859}{4104}k_{4,I} \right.\\
&\left. - \frac{11}{40}k_{5,I}\right)\Big\}\\
k_{6,R} = h * \Big\{ &(\gamma+\theta_3\sigma)\left(I_i - \frac{8}{27}k_{1,I} + 2k_{2,I} - \frac{3544}{2565}k_{3,I} + \frac{1859}{4104}k_{4,I} - \frac{11}{40}k_{5,I}\right)\\
&- \mu\left(R_i - \frac{8}{27}k_{1,R} + 2k_{2,R} - \frac{3544}{2565}k_{3,R} + \frac{1859}{4104}k_{4,R} - \frac{11}{40}k_{5,R}\right)\Big\}
\end{aligned} \tag{10}$$

4. Results and Discussion

For simulations, we take initial values of the variables listed in Table 1 and parameters in Table 2. We take two different parameters θ_1 which are $\theta_{1_s} = 0.9$ and $\theta_{1_e} = 0.7$. Parameter $\theta_{1_s} = 0.9$ leads to a reproduction number R_0 smaller than 1, whereas $\theta_{1_e} = 0.7$ results in a reproduction number R_0 greater than 1.

Table 1. Variables and their initial values

Variables	Initial values
$S(0)$	100
$E(0)$	15
$I(0)$	20
$R(0)$	4

Table 2. Parameters and their values

Parameters	Values
Λ	10
β	0.2
θ_{1_s}	0.9
θ_{1_e}	0.7
θ_2	0.1
θ_3	0.3
μ	0.3
δ	0.3
γ	0.2
σ	0.2

1. For $R_0 < 1$, it can be obtained using $\theta_1 = \theta_{1_s} = 0.9$, that is,

$$R_0 = \frac{\Lambda\beta(1-\theta_{1_s})[\delta + \theta_2(\gamma+\sigma+\mu)]}{\mu(\gamma+\sigma+\mu)(\delta+\mu)} = 0.5873 < 1$$

Because reproduction number $R_0 < 1$, the system converges to a disease free equilibirum:

$$\mathcal{E}^0 = (S^0, E^0, I^0, R^0) = \left(\frac{\Lambda}{\mu}, 0,0,0\right) = \left(\frac{10}{0.3}, 0,0,0\right) = (33.33,0,0,0)$$

Simulation results for this case $R_0 < 1$ using the RKF45 method is shown in Figure 2. We observe that for this case, as time t gets large, the system contains only the Susceptible subpopulation S.

2. For $R_0 > 1$, it can be obtained using $\theta_1 = \theta_{1_e} = 0.7$, that is,

$$R_0 = \frac{\Lambda\beta(1-\theta_{1_e})[\delta + \theta_2(\gamma+\sigma+\mu)]}{\mu(\gamma+\sigma+\mu)(\delta+\mu)} = 1.761 > 1$$

Because reproduction number $R_0 > 1$, the system converges to an endemic equilibrium:

$$\mathcal{E}^* = (S^*, E^*, I^*, R^*)$$

where

$$S^* = \frac{(\gamma+\sigma+\mu)(\delta+\mu)}{\beta(1-\theta_{1_e})[\delta+\theta_2(\gamma+\sigma+\mu)]} = 18.918$$

$$E^* = \frac{\Lambda}{(\delta+\mu)} - \frac{\mu(\gamma+\sigma+\mu)}{\beta(1-\theta_{1_e})(\delta+\theta_2(\gamma+\sigma+\mu))} = 7.207$$

$$I^* = \delta\left(\frac{\Lambda}{(\delta+\mu)(\gamma+\sigma+\mu)} - \frac{\mu}{\beta(1-\theta_{1_e})(\delta+\theta_2(\gamma+\sigma+\mu))}\right) = 3.088$$

$$R^* = \left(\frac{\Lambda\delta(\gamma+\theta_3\sigma)}{\mu(\delta+\mu)(\gamma+\sigma+\mu)} - \frac{\delta(\gamma+\theta_3\sigma)}{\beta(1-\theta_{1_e})(\delta+\theta_2(\gamma+\sigma+\mu))}\right) = 2.676$$

Simulation results for this case $R_0 > 1$ using the RKF45 method is shown in Figure 3. We observe from this figure that as time evolves, the Infected subpopulation I does not vanish. This means the disease exists in the system all the time.

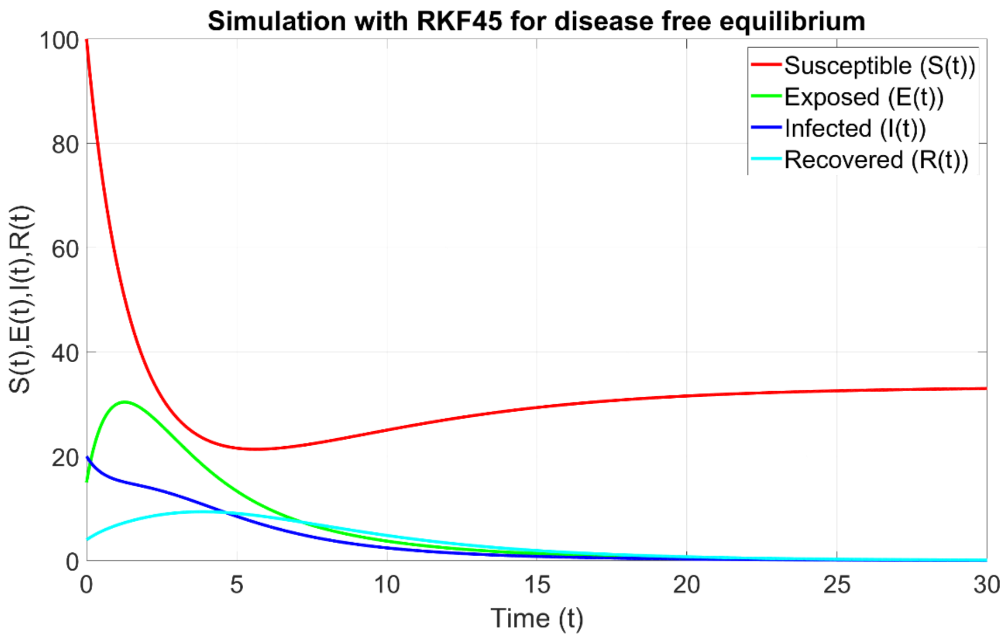

Figure 2. Simulation results using the RKF45 method for the case of disease-free equilibrium

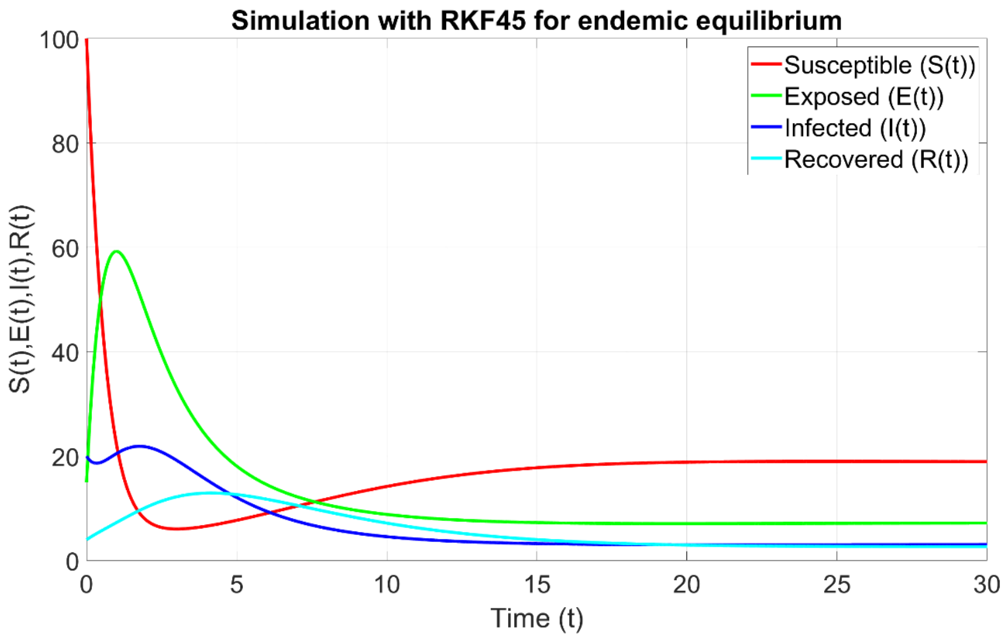

Figure 3. Simulation results using the RKF45 method for the case of endemic equilibrium

Now we shall report the main results of our research. To do so, we recall the formula of the order of accuracy for the numerical method [14]:

$$R_i = \frac{\log\left(\frac{\text{Error}_i}{\text{Error}_{i+1}}\right)}{\log\left(\frac{\Delta t_i}{\Delta t_{i+1}}\right)}$$

where Error_i is the average error, Δt_i is the time step $h = \Delta t_i$ and $i = 0,1,2,\dots,n$. Note that the exact solution to the SEIR model is not known until when this paper is written, so we use ODE45 of the MATLAB software as our reference solution. When ODE45 function is used, we set the AbsTol and RelTol both to be 10^{-13}.

1. For $R_0 < 1$

For the case of disease-free equilibrium, we record the average absolute and average relative errors and report the orders of accuracy based on these errors. Tables 3-6 provide the errors and orders of accuracy for Susceptible, Exposed, Infected, and Recovered subpopulations. We observe that the orders of accuracy converge to five as the time step gets small.

Table 3. Order of Accuracy of RKF45 for *Susceptible S* with $R_0 < 1$.

h	Absolute error	Relative error	Order of accuracy based on absolute error	Order of accuracy based on relative error
0.8	6.601E-03	2.078E-04	-	-
0.4	3.581E-05	1.242E-06	7.526	7.387
0.2	3.794E-07	1.176E-08	6.561	6.721
0.1	1.058E-08	2.415E-10	5.164	5.606
0.05	3.395E-10	6.938E-12	4.962	5.122
0.025	1.088E-11	2.160E-13	4.963	5.005

Table 4. Order of Accuracy of RKF45 for *Exposed E* with $R_0 < 1$.

h	Absolute error	Relative error	Order of accuracy based on absolute error	Order of accuracy based on relative error
0.8	2.998E-03	1.569E-04		
0.4	4.618E-06	7.021E-07	9.343	7.805
0.2	5.063E-07	2.779E-08	3.189	4.659
0.1	1.874E-08	9.079E-10	4.755	4.936
0.05	6.084E-10	2.834E-11	4.945	5.001
0.025	1.921E-11	8.826E-13	4.985	5.005

Table 5. Order of Accuracy of RKF45 for *Infected I* with $R_0 < 1$.

h	Absolute error	Relative error	Order of accuracy based on absolute error	Order of accuracy based on relative error
0.8	2.208E-03	2.239E-04	-	-
0.4	3.003E-05	2.684E-06	6.200	6.383
0.2	6.169E-07	5.041E-08	5.605	5.735
0.1	1.581E-08	1.238E-09	5.286	5.348
0.05	4.500E-10	3.460E-11	5.135	5.161
0.025	1.344E-11	1.025E-12	5.064	5.076

Table 6. Order of Accuracy of RKF45 for *Recovered R* with $R_0 < 1$.

h	Absolute error	Relative error	Order of accuracy based on absolute error	Order of accuracy based on relative error
0.8	1.267E-03	2.195E-04	-	-
0.4	1.205E-05	1.999E-06	6.716	6.779
0.2	1.985E-07	3.207E-08	5.924	5.962
0.1	4.640E-09	7.366E-10	5.419	5.444
0.05	1.274E-10	2.008E-11	5.187	5.197
0.025	3.756E-12	5.942E-13	5.084	5.079

2. For $R_0 > 1$

For the case of endemic equilibrium, again we record the average absolute and average relative errors and report the orders of accuracy based on these errors. Tables 7-10 contain the error values and orders of accuracy for Susceptible, Exposed, Infected, and Recovered subpopulations. Once again, we observe that the orders of accuracy tend to five as the time step approaches small values. However, the order of accuracy can be less than five if the time step is too small.

Table 7. Order of Accuracy of RKF45 for *Susceptible S* with $R_0 > 1$.

h	Absolute error	Relative error	Order of accuracy based on absolute error	Order of accuracy based on relative error
0.8	1.642E-01	9.527E-03	-	-
0.4	3.719E-04	1.407E-05	8.786	9.403
0.2	7.132E-06	4.746E-07	5.705	4.891
0.1	3.072E-07	1.802E-08	4.537	4.719
0.05	1.012E-08	5.778E-10	4.923	4.963
0.025	3.204E-10	1.810E-11	4.982	4.996

Table 8. Order of Accuracy of RKF45 for *Exposed E* with $R_0 > 1$.

h	Absolute error	Relative error	Order of accuracy based on absolute error	Order of accuracy based on relative error
0.8	1.536E-01	3.741E-03	-	-
0.4	4.914E-04	1.547E-05	8.288	7.918
0.2	1.211E-05	2.878E-07	5.342	5.748
0.1	3.944E-07	8.512E-09	4.941	5.079
0.05	1.210E-08	2.540E-10	5.027	5.066
0.025	3.728E-10	7.800E-12	5.020	5.026

Table 9. Order of Accuracy of RKF45 for *Infected I* with $R_0 > 1$.

h	Absolute error	Relative error	Order of accuracy based on absolute error	Order of accuracy based on relative error
0.8	3.679E-02	2.448E-03	-	-
0.4	3.303E-04	1.984E-05	6.799	6.947
0.2	4.927E-06	2.720E-07	6.067	6.189
0.1	1.042E-07	5.409E-09	5.563	5.652
0.05	2.688E-09	1.356E-10	5.277	5.318
0.025	7.700E-11	3.918E-12	5.126	5.113

Table 10. Order of Accuracy of RKF45 for *Recovered R* with $R_0 > 1$.

h	Absolute error	Relative error	Order of accuracy based on absolute error	Order of accuracy based on relative error
0.8	2.027E-02	1.954E-03	-	-
0.4	1.220E-04	1.225E-05	7.376	7.317
0.2	1.149E-06	1.318E-07	6.730	6.539
0.1	1.784E-08	2.425E-09	6.009	5.764
0.05	4.454E-10	6.525E-11	5.324	5.216
0.025	1.544E-11	2.166E-12	4.850	4.913

We obtain by simulations that the fifth-order RKF45 method is numerically verified that the numerical order of accuracy matches with the theoretical order of accuracy. Some variations may occur, that is, the numerical order of accuracy can be larger and smaller than five, as recorded in Tables 3-10. It can be larger than five for relatively large time-step variations, and smaller than five for relatively too small time-step variations.

5. Conclusion

We have verified numerically that the theoretically fifth-order RKF45 method achieved the order five when time step is sufficiently small. Larger numerical order of accuracy occurred in our simulations when time step is quite large. We note that large numerical order of accuracy is advantageous for solving initial value problems numerically if accuracy is more concerned than the speed of computation. This research is limited to numerical experiments. Future research direction could take numerical analysis of the errors of RKF45 when implemented to solve an SEIR model.

6. Acknowledgement

The authors thank Sanata Dharma University for the opportunity of this research. This paper is an improvement of a part of the first author's Bachelor of Mathematics (S.Mat.) thesis [15] written at Sanata Dharma University in 2024 under the supervision of the second author.

References

[1] Jana, A. K., *Numerical Methods: Theory and Engineering Applications,* Cambridge: Cambridge University Press, 2024.

[2] Mungkasi, S., *Matematika: Jalan Kesejahteraan,* Yogyakarta: Sanata Dharma University Press, 2022.

[3] Mathews, J. H., Fink, K. D., *Numerical Methods using MATLAB,* (Fourth Edition), Upper Saddle River: Prentice Hall, 2004.

[4] Jiao, J., Liu, Z., Cai, S., "Dynamics of an SEIR model with infectivity in incubation period and homestead-isolation on the susceptible," *Applied Mathematics Letters,* vol. 107, art. 106442, 2020.

[5] Palma, D. I., Mungkasi, S., "Fourth and fifth-order Runge-Kutta methods for solving a susceptible-exposed-infected-recovered mathematical model of the spread of COVID-19," *AIP Conference Proceedings,* vol. 3074, art. 020006, 2024.

[6] Rosari, F. I., Mungkasi, S., "Co-dynamics model of the spread of malaria and COVID-19 with numerical solutions using the third-orderand the fourth-order Runge-Kutta methods," *AIP Conference Proceedings,* vol. 3074, art. 020008, 2024.

[7] Setiawan, L. I., Mungkasi, S., "Penyelesaian model epidemi SIR menggunakan metode Runge-Kutta orde empat dan metode Adams-Bashforth-Moulton," *Komputasi: Jurnal Ilmiah Ilmu Komputer dan Matematika,* vol. 18, no. 2, pp. 55-61, 2021.

[8] Alkhazzan, A., Wang, J., Nie, Y., Khan, H., Alzabut, J., "A novel SIRS epidemic model for two diseases incorporating treatment functions, media coverage, and three types of noise," *Chaos, Solitons & Fractals,* vol. 181, art. 114631, 2024.

[9] Batiha, I. M., Ogilat, O., Bendib, I., Ouannas, A., Jebril, I. H., Anakira, N., "Finite-time dynamics of the fractional-order epidemic model: Stability, synchronization, and simulations," *Chaos, Solitons & Fractals: X,* vol. 13, art. 100118, 2024.

[10] Chen, B., Chen, R., Zhao. L., Ren, Y., Zhang, L., Zhao, Y., Lian, X., Yan, W., Gao, S., "High-resolution short-term prediction of the COVID-19 epidemic based on spatial-temporal model modified by historical meteorological data," *Fundamental Research,* vol. 4, no. 3, pp. 527-539, 2024.

[11] Esterhuizen, W., Sauerteig, P., Streif, S., Worthmann, K., "MPC without terminal ingredients tailored to the SEIR compartmental epidemic model," *Systems & Control Letters,* vol. 193, art. 105908, 2024.

[12] Guan, G., Guo, Z., Xiao, Y., “Dynamical behaviors of a network-based SIR epidemic model with saturated incidence and pulse vaccination,” *Communications in Nonlinear Science and Numerical Simulation,* vol. 137, art. 108097, 2024.

[13] Turkyilmazoglu, M., “Solutions to SIR/SEIR epidemic models with exponential series: Numerical and non numerical approaches,” *Computers in Biology and Medicine,* vol. 183, art. 109294, 2024.

[14] Hidayat, N., Suhariningsih, Suryanto, A., Mungkasi, S., “The significance of spatial reconstruction in finite volume methods for the shallow water equations,” *Applied Mathematical Sciences,* vol. 8, no. 29, pp. 1411-1420, 2014.

[15] Widi, L. K., *Model Matematis SEIR Pengaruh Isolasi Mandiri pada Kelompok Rentan dalam Penyebaran Penyakit Menular dan Penyelesaiannya dengan Metode RKF45 Orde Lima,* Skripsi (Bachelor’s Thesis), Yogyakarta: Sanata Dharma University, 2024.